

# Pore diameter-dependence photoluminescence spectra for porous anodized aluminum oxide membranes fabricated in different acid solutions

HONG-HOU LV<sup>a</sup> XUE-WEI WANG\*<sup>a,b</sup> YAO-REN KANG<sup>a</sup> ZHI-HAO YUAN<sup>a,c</sup>

<sup>a</sup>*School of Materials Science and Engineering, Tianjin University of Technology, Tianjin 300384, China*

<sup>b</sup>*Tianjin Key Laboratory for Photoelectric Materials and Devices, Tianjin University of Technology, Tianjin 300384, China*

<sup>c</sup>*Key Laboratory of Display Materials & Photoelectric Devices (Tianjin University of Technology), Ministry of Education, Tianjin 300384, China*

Porous anodized aluminum oxide (AAO) membranes with different diameters are fabricated using anodization of Al foils in the sulfuric acid, oxalic acid and phosphoric acid solutions. The photoluminescence (PL) properties of the corresponding AAO membranes are investigated. Based on morphology observations and PL measurements, it is revealed that the peak position of the observed PL band has an evident dependence on pore geometrical structure of AAO, and the PL spectra of AAO membranes are associated with the acid impurities and the singly ionized oxygen vacancies. The intensity change of PL bands for the acid impurities and the singly ionized oxygen vacancies is further discussed on the basis of the PL behavior of the AAO membranes with different pore-diameters. These results reveal that the PL properties of the AAO membranes are very sensitive to their chemical and pore-structures, which are closely related with their anodizing conditions. The present work may be helpful in understanding of the PL properties of the AAO membranes with different pore-diameters formed in different acid solutions.

(Received July 27, 2014; accepted April 05, 2016)

*Keywords:* Anodized aluminum oxide, Pore diameter, Photoluminescence, Oxygen vacancy

## 1. Introduction

The porous anodic aluminum oxide (AAO) membranes with highly ordered nanochannel array are formed by anodizing of Al foils in an appropriate acidic solution. In fact, these porous AAO membranes have the exceptional properties such as high pore density, ideal cylindrical shapes of the pores, controllable pore diameters, and very narrow distribution of pore sizes [1]. Due to its attractive properties, it is proposed as a promising template for the nanomaterial synthesis [2] such as nanorings [3-5], nanowires [6-9] and nanotubes [10-12]. Among these nanomaterials, many nanostructures have the excellent optical properties, which constitute a critical step in the development of operative nanometric devices. However, as far as we are concerned, the optical properties of the AAO itself have influence on the optical properties of materials fabricated based on the AAO membranes. Thus, it is necessary to study the self-properties of AAO for investigating the mechanisms of novel properties appearing in the composite materials synthesized using AAO membranes. Moreover, the research of the optical properties of AAO membranes is also crucial from the viewpoint of their technological applications as light emitting devices [13].

Recently, the optical properties of the AAO itself have been paid more attention to. These researches mainly focus on photoluminescence (PL) spectra as the basic information on the optical properties of AAO [14-20]. Gao et al. [15] and Li et al. [17] have demonstrated that the luminescent centers are originated from sulfuric and oxalic impurities incorporated into the porous oxide layer during anodization in oxalic and sulfuric acid electrolytes. The transformed carboxylic impurities related luminescence centers were found to be responsible for the luminescence characteristics of AAO membranes prepared by high field anodization process [21]. Furthermore, the researchers [22, 23] reported that the presence of oxygen vacancy related defect centers has also been attributed to the origin of visible PL in the AAO. These investigations show that the origin of the PL for AAO membranes depends on many factors, such as the nature of the electrolyte, conditions of the anodizing process [24], and their additional treatment (electrolytic or thermal) [25], etc. While, the change of these factors directly has effect on the pore structures of AAO, such as the diameter of pores. It is evident that the pore diameter of the AAO influences the characteristics of PL. Therefore, it is necessary to reveal the relation between pore diameter and PL of AAO. This is also especially

important with respect to the optical properties of AAO templates used for nanostructured optical devices. Despite enormous number of articles related to luminescence properties of porous oxide membranes formed by aluminum anodization in various electrolytes [26-32], there is a lack of data of the relation between the pore structure and luminescence properties of AAO membrane. The aim of this work is to study the PL properties of AAO membranes with different pore-diameters formed in the different electrolytes. The influence of pore diameter on the PL is investigated. This work can improve the understanding of the light-emitting property of the AAO with different pore-diameters.

## 2. Experimental

In our experimental, the AAO membranes were prepared by the conventional two-step anodization process as described previously [1, 33]. In short, high-purity aluminum foils (99.999%) were annealed in a vacuum of  $10^{-3}$  Pa at 500 °C for 5 h to remove the mechanical stress and obtain the homogenous structure. Then, the aluminum foils were electropolished in a mixture of perchloric acid and ethanol. The anodization of aluminum foils were conducted in different acid solutions (1.2 M  $H_2SO_4$ , 0.3 M  $H_2SO_4$ , 0.3 M  $H_2C_2O_4$ , or 0.1 M  $H_3PO_4$ ) under the constant-voltage condition. The detailed anodization conditions were given in the previous publication by the authors [33]. Anodization was carried out for 5 h with different kinds of acid solutions to form nanopores arrays with different diameters. After removing the alumina layer formed at the above step in a mixture of phosphoric acid (6 wt%) and chromic acid (1.5 wt%), the aluminum foils were oxidated again at the same conditions as the first step for 12 h. The remaining aluminum was etched by saturated  $CuCl_2$  solution. Meanwhile, for pore-widening treatment, the AAO membranes were kept in 5 wt% phosphoric acid solution at 30 °C to change the diameter of pores. After this process, the AAO membranes were dried at 60 °C to wipe off the water of surface.

The morphologies of the porous AAO membranes with different diameters were observed by field-emission scanning electron microscopy (FE-SEM: JEOL JSM-6700F). The PL spectra were taken using a Shimadzu (RF-5301) fluorescence spectrophotometer with a Xe lamp as the excitation light source. The excitation wavelength was 353 nm. All the measurements were carried out at room temperature.

## 3. Results and discussion

Fig. 1 shows the morphologies of the AAO membranes prepared in sulfuric acid, oxalic acid and phosphoric acid. It can be seen from Fig. 1 that the

average pore diameters of the AAO membranes are about 15, 20, 40, and 220 nm, respectively. The AAO membrane in Fig. 1a is anodized in 1.2 M  $H_2SO_4$  solution, and the pore diameter and pore distance are very small. The AAO membrane in Fig. 1b is anodized in 0.3 M  $H_2SO_4$  solution, and the pore diameter and pore distance are about 20 and 50 nm, respectively. The AAO membrane in Fig. 1c is anodized in 0.3 M  $H_2C_2O_4$  solution, and the pore diameter and pore distance are about 40 and 110 nm, respectively. Here, the pore diameter and pore distance all become bigger. The AAO membrane in Fig. 1d is anodized in 0.1 M  $H_3PO_4$  solution, and the pore diameter and pore distance are about 220 and 500 nm, respectively.

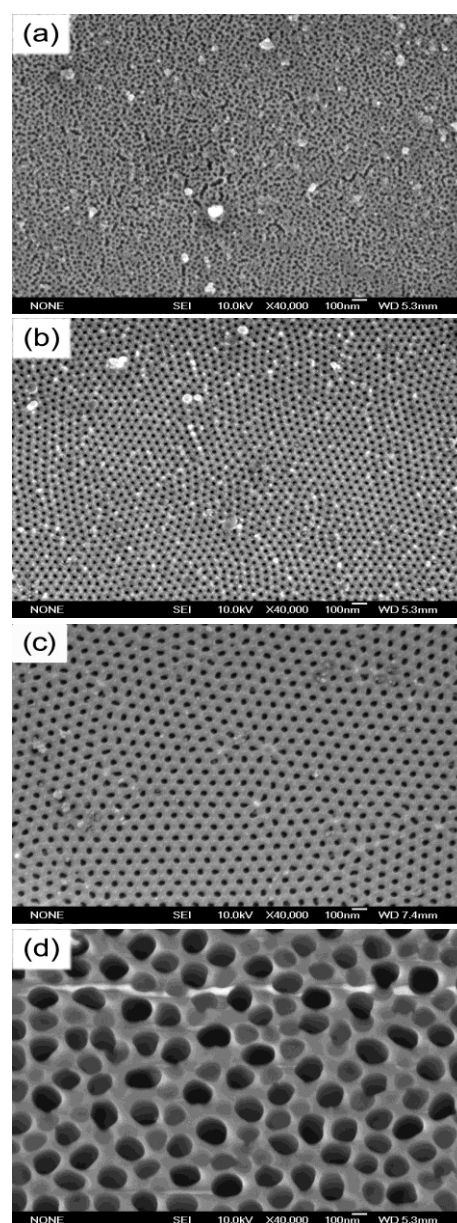


Fig. 1. SEM images of the AAO membranes with different pore-diameters: (a) 15 nm; (b) 20 nm; (c) 40 nm; (d) 220 nm.

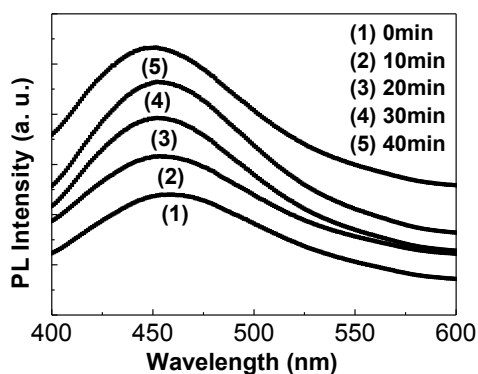


Fig. 2. PL spectra of the AAO membranes prepared in oxalic acid with different pore-widening treatment times.

Fig. 2 presents the PL spectra of AAO membranes prepared in oxalic acid, and these AAO membranes are etched in 5 wt% phosphoric acid solution for the different times. It can be seen from Fig. 2 that each PL spectrum appears as a broad emission (400-600 nm), which covers almost the whole visible waveband. While, the emission behaviors of the AAO membranes are obviously affected by etch-treatment. The PL intensity of the as-prepared sample is the lowest, and that of the sample etched for 30 min is the highest among five samples. With the increase of etching time, the position of PL peak for AAO membranes changes from 460 nm to 451 nm, which indicates that there exists a blue-shift of the peak position with the increase of pore diameters. Although the shift of peak-position is small by comparison with the width of the PL spectrum, it should be pointed out that the blue-shift of the PL spectra generally reflects a distribution of energy levels caused by different local environments of luminescent centers.

In order to know the mechanism of the PL emission, the PL spectra of AAO membranes prepared in oxalic acid are decomposed in several Gaussian distributions. It can be found from Fig. 3 that the PL spectra of AAO membranes have been deconvoluted by Gaussian functions into two emission bands. It can be seen from Fig. 3 that the intensity of two Gaussian fit peaks is different in each PL spectrum. These results suggest that two mechanisms might exist for the PL, and the PL spectra depend noticeably on the pore diameter. In generally, during the electrochemical growth of the AAO membrane, the compressive stresses and thermal energy produced at the aluminum/alumina interface can result in the formation of structural defects in the AAO membranes. Moreover, large numbers of double ionized oxygen vacancy could be also generated spontaneously in the AAO membranes when the oxygen ions migrate through the alumina layer towards the aluminum/alumina interface. If an electron is trapped in a double ionized oxygen vacancy during the electrochemical anodization, the singly ionized oxygen vacancy is formed, which is generally called  $F^+$  center.

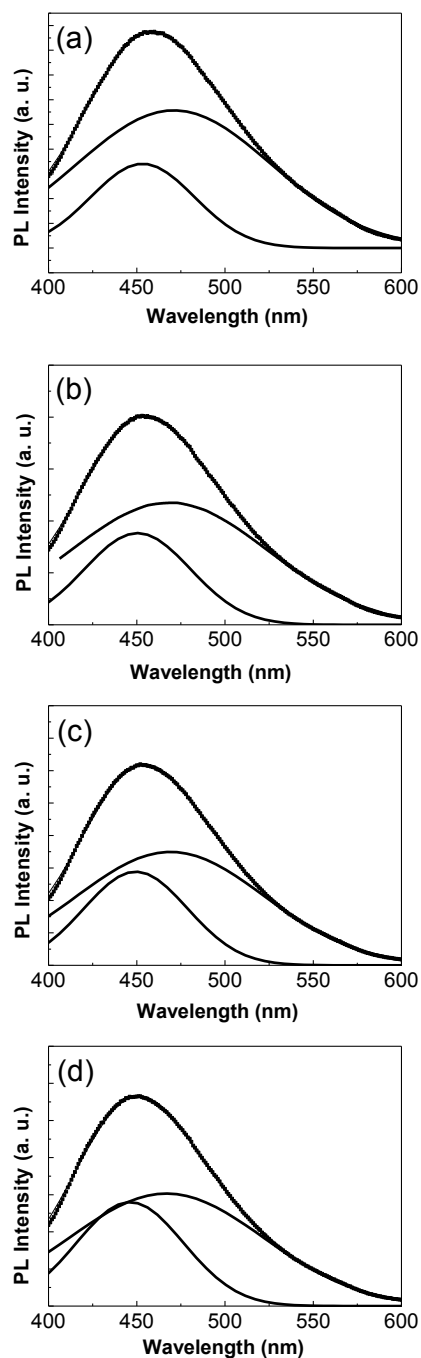


Fig. 3. The Gaussian fitting of emission spectra together with the changes of Gaussian fitting peak position for the AAO membranes prepared in oxalic acid with different pore-widening treatment times: (a) 0 min; (b) 10 min; (c) 30 min; (d) 40 min.

Some researchers thought that the PL spectra of AAO membranes were concerned to the singly ionized oxygen vacancies [13, 14, 34]. Additionally, the  $C_2O_4^{2-}$  ions from the electrolyte can also directly get incorporated in the membranes as impurities [17]. Yamamoto et al. [35] and Gao et al. [15] suggested that these oxalic impurities incorporated in the AAO membranes can be transformed into the luminescent centers via a high electric field setup inside the pore

walls, which shows a blue PL band around 470 nm. In our experimental, the present results in Fig.3 show that there are two Gaussian fit peaks in each PL spectrum. One peak is at the wavelength of about 469 nm, and another peak position is around the wavelength of 449 nm. This agreement makes us believe that the PL band at 469 nm originates from the oxalic impurities incorporated in the AAO membranes, and the PL band at about 449 nm may originate from  $F^+$  centers of AAO membranes. Therefore, the PL spectra of AAO membranes fabricated in oxalic acid are associated with the oxalic impurities and the singly ionized oxygen vacancies.

In the case of the different light-emitting point defects, the PL emission of each defect type contributes to the whole emission spectrum through a Gaussian-like peak. It is worth of noticing in Fig.3 that the intensity of two Gaussian fit peaks is different in each PL spectrum. For AAO membranes, the oxalic impurities incorporated during anodization are located predominantly in the outer region of the pore walls. With the increase of etch-treatment time, the oxalic impurities in the outer region of the pore walls decrease and the corresponding intensity of PL band also declines. While, the singly ionized oxygen vacancies in the AAO membranes are almost all located in the pore walls, and the corresponding intensity of PL band has not obvious change. Thus, with the increase of etch-treatment time, the intensity of PL band for the oxalic impurities decreases comparing with that for the singly ionized oxygen vacancies. This causes that the peak-position of the whole PL spectrum shifts toward the blue light with the increase of etch-treatment time (See Fig.2).

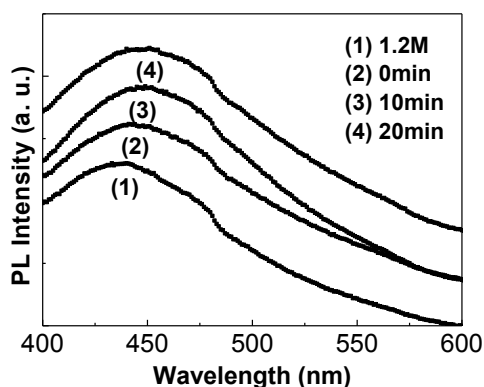


Fig. 4. PL spectra of the AAO membranes prepared in sulfuric acid with different pore-widening treatment times.

Fig. 4 presents the PL spectra of AAO membranes prepared in sulfuric acid. These PL spectra are corresponding to the samples without etch-treatment and those with the etching time  $t=10$  min and 20 min. It is observed that all the membranes show PL band in the

wavelength range of 400-600 nm, which covers almost the whole visible waveband. It can be seen that the emission behaviors of the AAO membranes are also affected obviously by etch-treatment. There exists a blue-shift of the peak position with increasing etching time. According to the above discussion of PL spectra, we know that the PL spectra of AAO membranes fabricated in oxalic acid are associated with the oxalic impurities and the singly ionized oxygen vacancies. Similarly, for the AAO membranes prepared in sulfuric acid, there are singly ionized oxygen vacancies in AAO. Compared with AAO membranes fabricated in oxalic acid, the quantity of singly ionized oxygen vacancies for AAO membranes prepared in sulfuric acid reduces because of lower anodization voltage, and the PL band of the sulfuric impurities moves toward the shorter wavelength [36]. Thus, Compared with AAO membranes fabricated in oxalic acid, the whole PL peak position of AAO membranes prepared in sulfuric acid moves toward the shorter wavelength. When the AAO membranes fabricated in sulfuric acid are etched in the 5 wt% phosphoric acid solution, the sulfuric impurities in the outer region of the pore walls decrease with the increase of etch-treatment time, and the corresponding intensity of PL band also declines. Therefore, the peak-position of the whole PL spectrum shifts toward the shorter wavelength with the increase of etch-treatment time. For the AAO membranes fabricated in 1.2 M sulfuric acid, the increase of sulfuric acid concentration leads to the increase of the sulfuric impurities, which causes the enhancement of PL band intensity. This make the whole PL position for the AAO membranes fabricated in 1.2 M sulfuric acid also shifts toward the shorter wavelength compared the PL position of AAO membranes prepared in 0.3 M sulfuric acid.

The PL spectrum of AAO membrane prepared in phosphoric acid is shown in Fig. 5. It can be seen from PL spectrum that PL band almost also covers almost the whole visible waveband, and the intensity of PL band weakens. By the discussion of PL spectra for AAO membranes fabricated in oxalic acid and sulfuric acid, we think that the PL spectrum of AAO membranes fabricated in phosphoric acid is also associated with the phosphoric impurities and the singly ionized oxygen vacancies. The corresponding AAO membrane is prepared in 0.1 M  $H_3PO_4$  under the voltage of 165 V, and the pore diameter is about 220 nm in Fig. 1, which has smaller surface area of pores compared with the AAO membranes fabricated in sulfuric acid and oxalic acid. Meanwhile, the decrease of phosphoric acid concentration leads to the decrease of the phosphoric impurities, which makes the corresponding intensity of PL band decline.

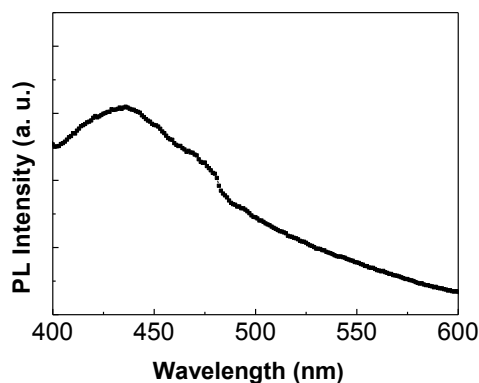


Fig. 5. PL spectrum of AAO membrane prepared in phosphoric acid.

#### 4. Conclusion

Porous AAO membranes with different diameters are successfully prepared via two-step anodization of high purity aluminum foils in the sulfuric acid, oxalic acid and phosphoric acid solutions. Their surface morphologies are characterized by using FE-SEM, and the pore diameter changes from 15 nm to 220 nm. The PL spectra of AAO membranes with different pore-diameters all show PL band in the wavelength range of 400-600 nm. It is found that both the acid impurities and the singly ionized oxygen vacancies can affect the PL emissions of the AAO membranes. With the increase of the etch-treatment time, the quantity of acid impurities obviously decreases, which results in the decline of the corresponding PL band intensity. For AAO membranes prepared in the sulfuric acid, the whole PL peak position moves toward blue light. While, for AAO membranes prepared in the oxalic acid, the whole PL peak position moves toward red light. For AAO membranes prepared in the phosphoric acid, the intensity of PL peak relatively weak because the AAO membranes have smaller surface area of pores. Our results show the pore diameter of AAO membranes adjusted by anodizing parameters has a significant influence on PL of AAO membranes. Therefore, PL investigations could be helpful for the further study on the interesting properties of the composite materials based on the AAO membranes.

#### Acknowledgements

This work was supported by the National Natural Science Foundation of China (No. 21171128) and Training Programs of Innovation and Entrepreneurship for Undergraduates (No. 201510060049).

#### References

- [1] A. P. Li, F. Müller, A. Birner, K. Nielsch, U. Gösele, *J. Appl. Phys.*, **84**, 6023 (1998).
- [2] X. W. Wang, Z. C. He, Z. H. Yuan, *Curr. Nanosci.*, **8**, 801 (2012).
- [3] S. Zhao, H. Roberge, A. Yelon, T. Veres, *J. Am. Chem. Soc.*, **128**, 12352 (2006).
- [4] K. L. Hobbs, P. R. Larson, G. D. Lian, J. C. Keay, M. B. Johnson, *Nano Lett.*, **4**, 167 (2003).
- [5] S. Wang, G. J. Yu, J. L. Gong, Q. T. Li, H. J. Xu, D. Z. Zhu, Z. Y. Zhu, *Nanotechnology*, **17**, 1594 (2006).
- [6] G. Sauer, G. Brehm, S. Schneider, K. Nielsch, R. B. Wehrspohn, J. Choi, H. Hofmeister, U. Gösele, *J. Appl. Phys.*, **91**, 3243 (2002).
- [7] X. W. Wang, Z. C. He, J. S. Li, Z. H. Yuan, *J. Alloys Compd.*, **595**, 221 (2014).
- [8] M. Koohbor, S. Soltanian, M. Najafi, P. Servati, *Mater. Chem. Phys.*, **131**, 728 (2012).
- [9] X. H. Huang, G. H. Li, X. C. Dou, L. Li, *J. Appl. Phys.*, **105**, 084306 (2009).
- [10] F. F. Tao, M. Y. Guan, Y. Jiang, J. M. Zhu, Z. Xu, Z. L. Xue, *Adv. Mater.*, **18**, 2161 (2006).
- [11] J. Bachmann, J. Escrig, K. Pitzschel, J. M. M. Moreno, J. Jing, D. Görlitz, D. Altbir, K. Nielsch, *J. Appl. Phys.*, **105**, 07B521 (2009).
- [12] L. Li, S. S. Pan, X. C. Dou, Y. G. Zhu, X. H. Huang, Y. W. Yang, G. H. Li, L. D. Zhang, *J. Phys. Chem. C*, **111**, 7288 (2007).
- [13] J. P. Zou, Y. F. Mei, J. K. Shen, J. H. Wu, X. L. Wu, X. M. Bao, *Phys. Lett. A*, **301**, 96 (2002).
- [14] Y. Du, W. L. Cai, C. M. Mo, J. Chen, L. D. Zhang, X. G. Zhu, *Appl. Phys. Lett.*, **74**, 2951 (1999).
- [15] T. Gao, G. W. Meng, L. D. Zhang, *J. Phys. Cond. Matter.*, **15**, 2071 (2003).
- [16] X. Y. Sun, F. Q. Xu, Z. M. Li, W. H. Zhang, *J. Luminesc.*, **121**, 588 (2006).
- [17] Y. Li, C. W. Wang, L. R. Zhao, W. M. Liu, *J. Phys. D: Appl. Phys.*, **42**, 045407 (2009).
- [18] G. S. Huang, X. L. Wu, L. W. Yang, X. F. Shao, G. G. Siu, P. K. Chu, *Appl. Phys. A*, **81**, 1345 (2005).
- [19] H. Yan, P. Lemmens, D. Wulferding, J. Shi, K. D. Becker, C. Lin, A. Lak, M. Schilling, *Mater. Chem. Phys.*, **135**, 206 (2012).
- [20] G. G. Khan, A. K. Singh, K. Mandal, *J. Luminesc.*, **134**, 772 (2013).
- [21] Y. B. Li, M. J. Zheng, L. Ma, *Appl. Phys. Lett.*, **91**, 073109 (2007).
- [22] G. S. Huang, X. L. Wu, Y. F. Mei, X. F. Shao, G. G. Siu, *Appl. Phys. Lett.*, **93**, 582 (2003).
- [23] J. H. Chen, C. P. Huang, C. G. Chao, T. M. Chen, *Appl. Phys. A*, **84**, 297 (2006).
- [24] Z. Li, K. Huang, *J. Phys. Condens. Matter*, **19**, 216203 (2007).

- [25] S. Stojadinovic, Z. Nedic, I. Belca, R. Vasilic, M. B. Kasalica, M. Petkovic, L. Zekovic, *Appl. Surf. Sci.*, **256**, 763 (2009).
- [26] G. H. Li, Y. Zhang, Y. C. Wu, L. D. Zhang, *J. Phys. Condens. Matter*, **15**, 8663 (2003).
- [27] Y. F. Liu, Y. F. Tu, S. Y. Huang, J. P. Sang, X. W. Zou, *J. Mater. Sci.*, **44**, 3370 (2009).
- [28] A. Rauf, M. Mehmood, M. Ahmed, M. Hasan, M. Aslam, *J. Luminesc.*, **130**, 792 (2010).
- [29] S. Stojadinovic, R. Vasilic, Z. Nedic, B. Kasalica, I. Belca, L. Zekovic, *Thin Solid Films*, **519**, 3516 (2011).
- [30] A. Santos, M. Alba, M. M. Rahman, P. Formentín, J. Ferré-Borrull, J. Pallarès, L. F. Marsal, *Nanoscale Res. Lett.*, **7**, 228 (2012).
- [31] X. Wu, S. Xiong, J. Guo, L. Wang, C. Hua, Y. Hou, P. K. Chu, *J. Phys. Chem. C*, **116**, 2356 (2012).
- [32] A. Nourmohammadi, S. J. Asadabadi, M. H. Yousefi, M. Ghasemzadeh, *Nanoscale Res. Lett.*, **7**, 689 (2012).
- [33] X. W. Wang, G. T. Fei, X. J. Xu, Z. Jin, L. D. Zhang, *J. Phys. Chem. B*, **109**, 24326 (2005).
- [34] Y. Li, G. H. Li, G. W. Meng, L. D. Zhang, F. Phillipp, *J. Phys. Condens. Matter*, **13**, 2691 (2001).
- [35] Y. Yamamoto, N. Baba, S. Tajima, *Nature*, **289**, 572 (1981).
- [36] J. Wang, C. W. Wang, S. Y. Li, F. Zhou, *Appl. Phys. A*, **94**, 939 (2009).

---

\*Corresponding author: xwwang@tjut.edu.cn